Construction and Building Materials 125 (2016) 873–883

Contents lists available at ScienceDirect

Construction and Building Materials

journal homepage: www.elsevier.com/locate/conbuildmat

# Effects of nanoclay and nanocomposites on bitumen rheological properties

Luísa Gardênia A.T. Farias [a], Janaina L. Leitinho [c], Bruno de C. Amoni [b], Juceline B.S. Bastos [c], Jorge B. Soares [c], Sandra de A. Soares [b], Hosiberto B. de Sant'Ana [a,*]

[a] Dept. of Chemical Engineering, UFC, Fortaleza, Brazil
[b] Dept. of Organic and Inorganic Chemistry, UFC, Fortaleza, Brazil
[c] Dept. of Transportation Engineering, UFC, Fortaleza, Brazil

## HIGHLIGHTS

- SBS modified bitumen prepared in the laboratory presented phase separation.
- Cloisite nanoclay improves storage stability of SBS modified bitumen.
- The additives improve the resistance to rutting and elasticity of the bitumen.
- SBS/nanoclays support a Standard traffic.

## ARTICLE INFO

*Article history:*
Received 30 July 2015
Received in revised form 19 August 2016
Accepted 28 August 2016

*Keywords:*
SBS/nanoclay modified bitumen
Organo montmorillonite
Rheological properties

## ABSTRACT

Nanoclays have been successfully introduced into the asphalt, either separated or in the form of polymer/bitumen blends, improving mechanical and rheological properties. In this paper, the organoclay montmorillonite (OMMT) was prepared to be used as an additive for bitumen and for a polymer modified bitumen. A nanoclay Cloisite® 20 Å (CLO), was also investigated for comparison purposes. A bitumen was modified with 4% nanoclays (OMMT and CLO), with 4% SBS, and with 4% SBS/nanoclay. All modified bitumens (MB) exhibited higher G* and lower δ, indicating an improvement in the stiffness and in the elasticity. SBS/Nanoclay MB presented similar rheological behavior compared to SBS MB which may result in cost savings. The addition of SBS and SBS/OMMT resulted in increase in PG grade and decrease in non-recoverable creep compliance ($J_{nr}$) indicating a better rut resistant compared to pure bitumen.



## 1. Introduction

Bitumen has been widely used in paving applications because of its physical and rheological properties, including also adhesive and impermeability capabilities. It is the most suitable material to provide a protective coating and to act as a binder to aggregates. However, due to mechanical and environmental loads, bitumen tends to exhibit fatigue damage, rutting, and thermal cracking. Therefore, its modification is often needed to improve properties. Modifiers such as polymers provide the properties needed for higher performance pavements [1–3]. Polymer modified asphalt pavements exhibit greater resistance to rutting, resistance to low temperature cracking, fatigue, and decrease in thermal susceptibility.

The styrene butadiene styrene (SBS) triblock copolymer is one of the most successful polymers used in the pavement industry. It can exhibit higher resistance to rutting, stripping and low thermal susceptibility in a wide range of temperatures [1]. Researches indicate that the addition of polymers (0.3–1%) resulted in increased reduction (approximately 90%) in the emissions of benzene [4]. The polymeric phase dispersed in the bitumen surface acts as a protective layer, minimizing the emission of the substances. The major problem of SBS modified bitumen is the possible phase separation during prolonged storage at high temperatures. The cause of the instability is attributed to the density difference between SBS polymer and bitumen [6]. However, recent progress in the asphalt industry has led to many commercial preblended SBS modified asphalt that can be stored for a reasonable amount of time without any separation problem. Nevertheless, polymer modification within the laboratory often present phase separation.

* Corresponding author at: Departamento de Engenharia Química, Universidade Federal do Ceará, Campus do Pici, Bloco 709, 60455-760 Fortaleza – CE, Brazil.
*E-mail address:* hbs@ufc.br (H.B. de Sant'Ana).

http://dx.doi.org/10.1016/j.conbuildmat.2016.08.127
0950-0618/

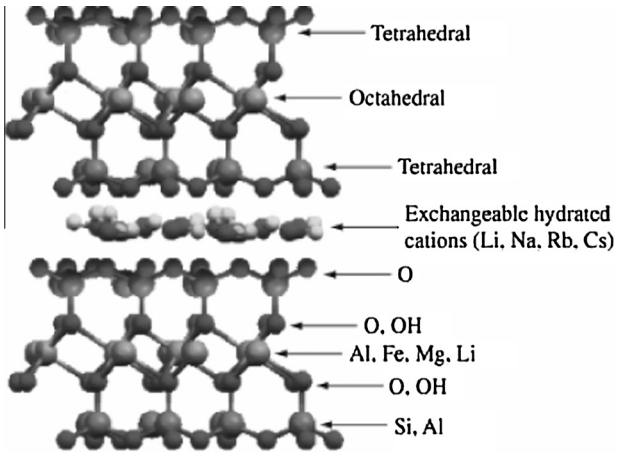


**Fig. 1.** Silicate layers: two tetrahedrally coordinated silicon atoms fused [8].

With the development of nanotechnology, layered silicate nanoparticles became a new material to be used as an additive for asphalt cement [6]. The use of nanoclay as filler and polymer/clay nanocomposite has shown to improve pavement performance [5]. In addition, it contributes to an increasing compatibility between the bitumen and the polymer, given that the presence of the clay seems to reduce the difference between the density of the polymer and the bitumen, therefore improving storage stability [6,7].

It is expected that the clay mineral alone or dispersed in the polymer modified bitumen can exhibit superior physical, mechanical and barrier properties when compared to conventional asphalt [8–13]. These improvements can include high moduli, heat resistance [14], decreased gas permeability [15–19], and flammability [20–24], alternative to reduce the processing temperature and the emission of volatiles.

The commonly used clay mineral or layered silicates for the preparation of clay modified bitumen as nanocomposites belong to the general family of 2:1 phyllosilicates. Typical clays include Kaolinite (KC) [25], fluorohectorite [24], vermiculite and montmorillonite (MMT) [26]. The clay minerals consist of aluminum silicate layers: silica $SiO_4$-tetrahedron bonded to alumina $AlO_6$-octahedron. The tetrahedral and octahedral parts can fit within themselves to form layers in various ways, resulting in different crystalline structures.

Clay layers are negatively charged but stay together due to the presence of the positive ion (for example $Na^+$, $Mg^{++}$, and $Al^{+++}$) between the clay layers (Fig. 1). This layered silicate is characterized by a surface charge known as cation exchange capacity (CEC), expressed as meq per 100 g clay [27]. Montmorillonite, a natural layered clay, is one of the most studied clays due to its non-toxicity and high cation exchange capacity [28].

It is important to mention that in order to render layered silicates miscible with polymers or other thermoplastic material such as bitumen, they have to be modified by surface treatment to produce organophilic clay resulting in a larger interlayer spacing [29,30]. Separation of the clay layers results in a nanoclay with a large active surface area (700–800 $m^2\,g^{-1}$) [11]. Intercalation of polymers or other matrix, including bitumen, results in micro or nanocomposites [27,31,32] with a large field of applications [33,34]. The dispersion of the clay in the matrix can form different types of structure (Fig. 2).

Microcomposite structures are formed when the material does not intercalate between the clay layers, resulting in a composite with phase separation. The nanocomposite structures can be classified into two main groups: intercalated or exfoliated. In the first case, the multi-layer of the clay is maintained after the intercalation of the polymers and the spacing between individual layers increase. In the exfoliated structure the layered structure of the clay is disrupted and uniformly distributed in the matrix [30]. Clay nanocomposites can be obtained mainly by the three following methods: melt process intercalation, in-situ polymerization, and solution blending [27].

In this paper, two types of organomodified MMT were used as additives in bitumen modification – a natural one and the nanoclay Cloisite® 20 Å – a commercial organo modified montmorillonite. The effect of organoclay modification in pure and SBS modified bitumen was studied to evaluate physical and rheological parameters correlated to pavement performance. In previous work, triple nanocomposites – a physical blend of bitumen/SBS/nanoclays – were studied, in which the intercalation in the clay layers is mainly due to bitumen molecules [26]. In the present work, a nanocomposite is formed in a different way. The polymer is first premixed with the clay in order to favor polymer intercalation between the clay layers producing a polymer/nanoclay composite by a solution intercalation method, before bitumen modification. This study is useful to better understand the behavior and properties of the nanostructure in bitumen modification, aiming to its broad use in pavement engineering.

## 2. Experimental program

### 2.1. Materials

A bitumen classified as a 50/70 penetration grade was provided by the Petrobras/Lubnor refinery. The linear SBS copolymer speci-

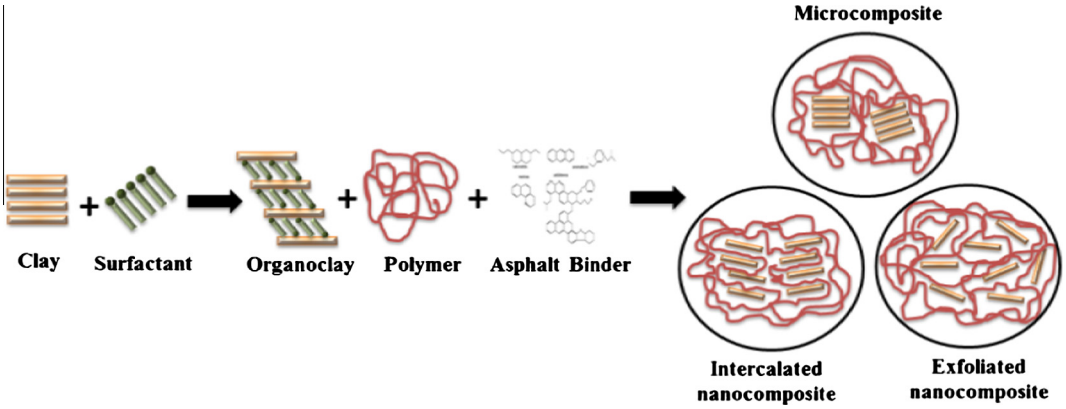


**Fig. 2.** Schematically illustration of three different types of thermodynamically achievable polymer/layered silicate nanocomposites. Types of microstructures of polymer clay composites: a) microcomposites, b) intercalated nanocomposite, and c) exfoliated nanocomposite.

fied as type 1110 was supplied by Kraton. The nanoclay Cloisite® 20 Å supplied by Southern Clay Products INC. (US) is a commercial montmorillonite treated with an organic salt modifier (dimethyl, dehydrogenated tallow, quaternary ammonium-2M2HT), with X-ray result$d_{001}$ = 20 Å, with a cation exchange capacity (CEC) of 95 meq per 100 g, as indicated by the suppliers. The montmorillonite was provided by Mineração Vale do Juquiá Ltda, Brazil. The surfactant used for the organophilization of the montmorillonite was CETREMIDE (cetyltrimethyl ammonium bromide) and it was supplied by Vetec/Brazil.

### 2.2. Clay modification

The clay suspension was prepared by adding 20 g of MMT–$Na^+$ into 500 mL of water to ensure swelling of the clay. It was kept for 24 h and then stirred for 5 min in a Sonifier® Model W-450 D-50% amplitude at room temperature. The organically modified montmorillonite (OMMT) was prepared by ion exchange reaction of MMT-$Na^+$ with an organic salt CETREMIDE. The suspension was stirred for 2 h. Then it was centrifuged at 6000 rpm for 6 min. The precipitate was then washed with distilled water and centrifuged again at the same condition, which was repeated several times to make it free from CETREMIDE excess. Hence, the final paste of organo montmorillonite (OMMT) was obtained. The paste was oven-dried (70 °C, overnight) into powder for later use.

### 2.3. Preparation of nanocomposites

The nanocomposites were prepared by the solution intercalation method. A desired amount of OMMT (5% by weight of the SBS) was dispersed in toluene at room temperature for 24 h under stirring. The SBS was also dissolved in toluene and homogenized in another recipient for 24 h. Toluene is an appropriate substance because it is an organic solvent which dissolves SBS easily and at the same time allows exfoliation of the nanoclay.

Both solutions were mixed and kept under stirring for 24 h. Subsequently, the final solution was poured into a Petri-dish and dried at room temperature to remove any solvent. After the solvent was completely removed, the composite polymeric film was taken out and dried for further analyses.

### 2.4. Preparation of the organoclays modified bitumen; SBS modified bitumen and SBS/organoclays nanocomposite modified bitumen

All samples were prepared by means of a high shear mixer – Silverson model L4R, at 2000 rpm. The conventional bitumen (B) was heated to a temperature of 160 °C. The additives were then added slowly to the bitumen. The rotation was maintained for 2 h after the physical mixture of the additives, while keeping the temperature at 160 °C. The SBS/nanoclay composites were added (4% by weight of the binder). The modified bitumens (MB) considered in this study are:

(i) Conventional bitumen (B);
(ii) B modified by 4% OMMT (OMMT MB);
(iii) B modified by 4% Cloisite® (CLO MB);
(iv) B modified by 4% of SBS (SBS MB);
(v) B modified by 4% of SBSOMMT (SBSOMMT MB);
(vi) B modified by 4% of SBSCLO (SBSCLO MB).

### 2.5. Cation Exchange Capacity (CEC)

The method of ammonium acetate saturation (AMAS) is commonly used to measure the CEC of finely crystalline materials [35]. The AMAS method involves the saturation of the MMT with ammonium ($NH_4^+$) ions that replace exchangeable cations. The number of $NH_4^+$ ions retained by the MMT is a measure of the CEC. The determination procedure for the CEC used herein was similar to the referred one [36]. The cation-exchange CEC of Cloisite® clay is according to Products Bulletin from Southern Clay.

### 2.6. X-ray diffraction

The X-ray diffractogram was obtained using a PAN analytical X-ray diffractometer with geometry and mirror monochromator of cobalt radiation with a wavelength 1.78896 Å. The basal spacing of nanoclays was estimated from the position of the ($d_{001}$) peak and calculated using Bragg's law (Eq. (1)):

$$2d_{001}\sin\theta = n\gamma \quad (1)$$

where, $d_{001}$: spacing between the planes in the atomic lattice, $\theta$: angle between the X-ray and the scattering planes, $n$: is an integer, and $\lambda$: the wavelength of X-ray wave.

### 2.7. Viscosity test

The viscosity of the bitumens was measured with a Brookfield DV-II+ rotational viscometer with a THERMOSEL control system according to ASTM standardD4402 [37]. Measurements were taken at 135, 150 and 175 °C. Two different spindles were used: SC4-21 and SC4-27, for the unmodified and modified bitumens, respectively. The samples were submitted to shear rates of 2.5, 5, 10, 20, 30 and 40 rpm. The dependence of viscosity on temperature was used to obtain the flow activation energy ($E_f$) as indicated in Eq. (2) from the Arrhenius-like equation:

$$\log(\eta) = E_f/RT + \ln A \quad (2)$$

where $\eta$: viscosity of the material at 20 rpm, T: temperature in Kelvin, A: pre-exponential factor, $E_f$: flow activation energy, and R: universal gas constant (8.314 J $mol^{-1}$ $K^{-1}$). Upon plotting $\ln\eta$ as a function of 1/T, from the slope it is possible to obtain values of $E_f$/R. The parameter $E_f$ has been used to differentiate bitumens and rank their thermal susceptibility.

### 2.8. Conventional physical test

The pure and modified asphalt binders were subjected to the following empirical tests: penetration (PEN) and softening point (SP). The first was performed using a penetrometer semi-automatic, according to ASTM standardD5 [38]. Penetration is the depth, in tenths of a millimeter that a 100 g standard needle penetrates into a sample after 5 s at a temperature of 25 °C. The softening point (ring and ball method) aims to determine the temperature at which the asphalt binder reaches a certain flow condition when heated under certain standard conditions, according to ASTM D36/D36M [39]. Three measurements were obtained for each sample.

### 2.9. Rheological Tests by Dynamic Shear Rheometer (DSR)

The rheological tests for the samples were performed in a dynamic shear rheometer (DSR), model TA AR 2000®. Frequency sweep tests (from 0.01 to 100 Hz) were applied under a controlled-stress of 120 Pa according to ASTM D7175 [40]. Measurements were performed within the linear viscoelastic region. The tests were conducted in two different temperature ranges: −10 to 40 °C (first stage), and 40–85 °C (second stage). The samples were prepared in a silicon mold 2 mm thick and 8 mm diameter for the first stage, and 1 mm thick and 25 mm diameter for the second stage. The linear viscoelastic parameters obtained were: complex shear modulus ($G^*$) and phase angle ($\delta$). The rheological response in the viscoelastic region was represented by master curves of their

**Table 1**
Classification MSCR.

| MSCR | Limits $J_{nr3200}$ (a) | MSCR | ESAL (b) |
|---|---|---|---|
| $J_{nr3200}$; $kPa^{-1}$ $J_{nrdiff}$ < 0.75 | ⩽4.5 $kPa^{-1}$ | S – Standard | <10 million |
| | ⩽2.0 $kPa^{-1}$ | H – Heavy | >10 million |
| | ⩽1.0 $kPa^{-1}$ | V – Very Heavy | >30 million |
| | ⩽0.5 $kPa^{-1}$ | E – Extreme | >30 million* |

(a) [49]; (b) [50]; (*) and standing traffic.

viscoelastic functions. The Time-Temperature Superposition Principle (TTSP) [41] was applied using the well-known Williams-Landel-Ferry (WLF) equation [42]. The reference temperature was chosen to be 25 °C.

*2.9.1. Multiple Stress Creep Recovery tests (MSCR)*

Multiple Stress Creep Recovery tests (MSCR) were performed after the aging of samples in short term and maximum PG temperature. A total of 10 cycles of creep and recovery – 1 s load and 9 s recovery – at 100 Pa was applied in the asphalt binder sample between the two parallel plates of the DSR (25.0 mm in diameter and 1.0 mm spacing between plates) followed by other 10 cycles at 3200 Pa [46]. The percentage of recovery (R) and non-recoverable creep compliance ($J_{nr}$) were calculated for all cycles at 100 and at 3200 Pa, and the final results for both parameters correspond to the arithmetic average of the respective values. The percentage differences between the non-recoverable creep compliance ($J_{nr,diff}$) were calculated by Eq. (3).

$$J_{nr,diff} = \left[\frac{(J_{nr}3200 - J_{nr}100)}{J_{nr}100}\right] \cdot 100 \quad (3)$$

$J_{nr,diff}$: difference between the non-recoverable creep compliances at two different stress levels (%); $J_{nr}100$: non-recoverable creep compliance at 100 Pa ($Pa^{-1}$ or $kPa^{-1}$); and $J_{nr}3200$: non-recoverable creep compliance at 3200 Pa ($Pa^{-1}$ or k $Pa^{-1}$).

Asphalt binders were classified based on traffic volume, using the value of $J_{nr}$ as a parameter [46]. This parameter allows the evaluation of the resistance to rutting and it presents a good correlation with the mechanical tests on asphalt mixtures [47–50]. The classification is according to Table 1, where Equivalent Single Axle Load (ESAL) corresponds to the accumulated number of passes of a standard axle of 8.2 tons during the project life.

*2.9.2. Performance grade*

The Performance Grade (PG) categorizes the bitumen used in asphalt pavements relative to its rated performance at different temperatures. The DSR test was used to evaluate the binder properties at high and intermediate temperatures, which are related to rutting and fatigue cracking, respectively. The PG of these bitumens was determined according to Superpave testing protocols [43].

*2.9.3. Compaction and mixing temperatures by Casola's method*

The mixing temperature is defined as the temperature at which the aggregate can be sufficiently and uniformly coated. The compaction temperature is typically in the range of 135–155 °C (275–310°F), and based solely on the ability of the compaction equipment available to achieve adequate in-place density.

To determine the mixing and compaction temperatures of bitumen, the phase angle method developed by Casola was adopted [44]. The method consists of performing a frequency sweep in the bitumen using a DSR, according to Superpave PG testing requirements. Tests were conducted at 45–80 °C, and at shear frequency sweep from 0.01 to 100 rad/s. The data were collected to construct a master curve-time temperature superposition at a temperature of 80 °C. The phase angle of 86 °C is used to identify the frequency corresponding to bitumen transition, from a viscous behavior to a viscoelastic one. This frequency is used to calculate mixing and compaction temperatures according to equations 4 and 5, respectively.

$$\text{Mixing temperature } (^{\circ}\text{F}) = 325(\omega)^{-0.0135} \quad (4)$$

$$\text{Compaction temperature } (^{\circ}\text{F}) = 300(\omega)^{-0.012} \quad (5)$$

ω: frequency in rad/s.

*2.10. Storage stability test*

Storage stability tests of modified bitumen were performed according to ABNT 15166 [45]. The samples were transferred into an aluminum toothpaste tube (25 mm in diameter and 147 mm in height) and stored at 163 °C for 48 h in an oven, and then at −6.7 °C for 4 h in a freezer. A piece of the sample was subsequently taken from the top and bottom of the tube, to be subjected to a frequency sweep test: 0.01–100 Hz under a controlled stress of 120 Pa at 25 °C. The logarithm of the ratio between G* of the bottom part and G* of the top part is defined as the separation index (Is). The closer to zero this parameter is, the better is the storage stability of the bitumen. This test helps to assess the miscibility of the polymer and the bitumen, which is critical for storage at high temperature.

## 3. Results and discussion

*3.1. Properties of organomodified clays*

The properties of organomodified clays are presented in Table 2. The cation exchange capacity (CEC) data from MMT was calculated by the methods of ammonium acetate saturation (Section 2.5). [36] According to the Bulletin from Southern Clay Products Inc., Gonzales, TX, the Cloisite® 20 Å presents CEC of 95 meq per 100 g clay. Table 2includes the basal spacing from X-ray result ($d_{001}$) (Figs. 3 and 4).

*3.2. Results for polymer/layered silicate nanocomposites formation by X ray diffraction (XRD)*

The XRD pattern of OMMT, SBSOMMT and SBSCLO nanocomposites are shown in Figs. 3–5. The X-ray powder diffraction (XRD) pattern of OMMT and MMT shows that the MMT characteristic peak ($d_{001}$) is 2θ = 8°. This peak refers to the basal spacing of 13 Å. As shown in Fig. 3a, the peak shifts to a lower angle (2θ = 5°), indicating an increase in basal spacing for 19 Å. Thus, it

**Table 2**
Typical Properties of OMMT and Cloisite® 20 Å.

| Organomodified Clay | OrganicModifier | Cation Exchange Capacity (CEC) | X-ray result ($d_{001}$) |
|---|---|---|---|
| Cloisite® 20 Å[a] | Dimethyl, dehydrogenated tallow, quaternary ammonium/2M2HT | 95 meq per 100 g clay | 24 Å |
| Organically modified montmorillonite | Bromide cetyltrimethyl-ammonium chloride | 94 meq per 100 g clay | 19 Å |

[a] Extracted from Southern Clay Products (www.scprod.com).

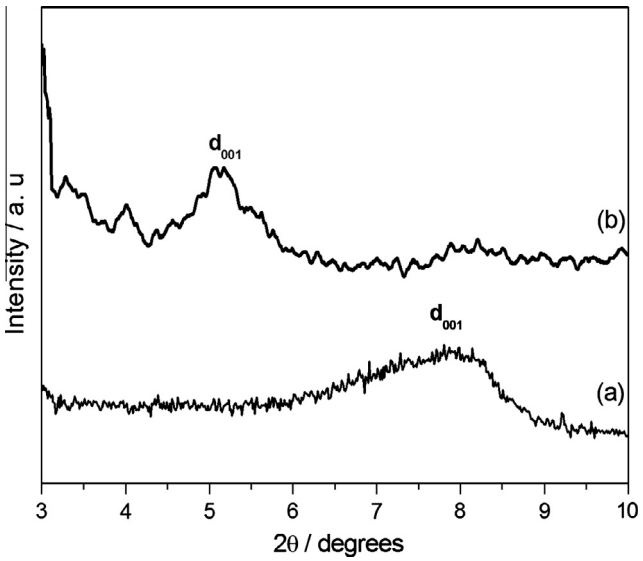


**Fig. 3.** X-ray diffractogram for (a) MMT and (b) OMMT.

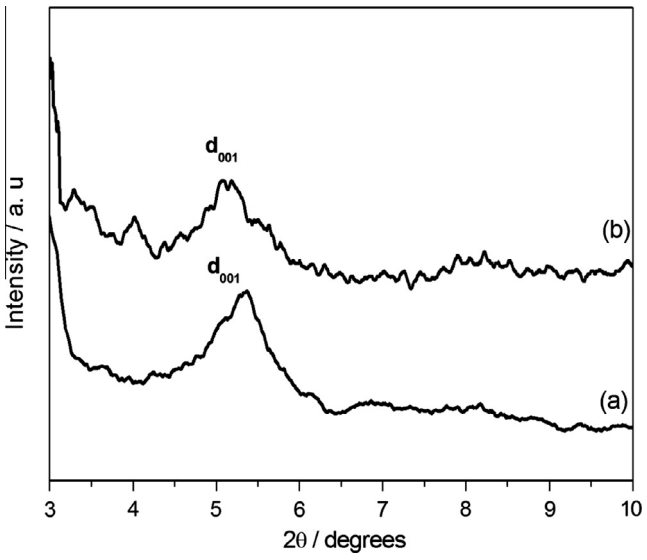


**Fig. 5.** X-ray diffractogram for (a) OMMT and (b) SBSOMMT nanocomposite.

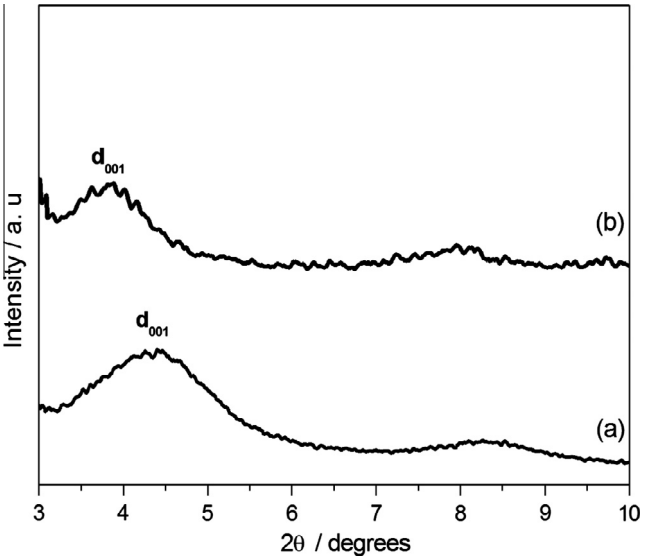


**Fig. 4.** X-ray diffractogram for (a) CLO and (b) SBSCLO nanocomposite.

indicated that after modification with CETREMIDE, the basal spacing is increased, which can be related to the incorporation of organic chains into the interlayer of the clay. Comparing the XRD pattern of CLO and OMMT, it is reasonable to assume that bitumen was more efficiently dispersed in the CLO interlayers than in the OMMT interlayers.

The XRD curves of CLO – SBSCLO and OMMT – SBSOMMT nanocomposites are shown in Figs. 4 and 5, respectively. The nanocomposites exhibit representative variation in XRD patterns when compared to the XRD pattern of nanoclays. For the XRD curves (Fig. 4a and b) of CLO and SBSCLO, it is observed a shift from $2\theta = 4.5°$ to a lower angle of $2\theta = 4°$. These peaks refer to the basal spacing of 24 Å and 27 Å, respectively. Therefore, the SBS was partially intercalated in the interlayer spacing. It is reasonable to assume that the organic salt was substituted for the polymer in some extension. For OMMT and SBSOMMT (Fig. 5a and b) the characteristic peak (d001) for OMMT presented a basal space of 19 Å, and for SBSOMMT a basal space of 20 Å. This result indicated that the nanoclay lamellas are not exfoliated in the polymer matrix, but dispersed forming a microcomposite. The microstructures of polymer/layered silicate nanocomposites can usually be classified into three categories: intercalated, exfoliated and microcomposites, which can be characterized using the XRD technique relying on the position and the intensity of diffraction peaks in the XRD patterns [45]. However, it will be shown that bitumen and SBS/nanoclays were somehow bonded so that no phase separation occurred.

### 3.3. Viscosity and conventional physical test

The results of viscosity, flow activation energy and physical test for all the samples are listed in Table 3. The effect of additives is quite clear in Fig. 6, which presents the viscosity as a function of temperature at 20 rpm shear rate. The viscosity dependence on shear rate can be observed in Fig. 7. As expected, the lowest temperature leads to higher viscosity. SBS/OMMT MB presented the highest viscosity values, probably due to the formation of an incompatible blend. The CLO and OMMT MBs also showed an

**Table 3**
Viscosity of 50/70 bitumen and modified bitumen, flow activation energy ($E_f$) and conventional physical test.

| Samples | Viscosity (Pa s) | | | $E_f$ (J/mol) | *SP* | *PEN* |
|---|---|---|---|---|---|---|
| | 135 °C | 150 °C | 175 °C | | | |
| 50/70 B | 0.548 | 0.263 | 0.100 | 56 | 50 | 61 |
| 4% SBS MB | 1.520 | 0.908 | 0.313 | 58 | 71 | 40 |
| 4% CLO MB | 0.721 | 0.353 | 0.143 | 61 | 60 | 58 |
| 4% OMMT MB | 0.985 | 0.648 | 0.343 | 37 | 53 | 51 |
| 4% SBSCLO MB | 1.325 | 0.700 | 0.300 | 56 | 52 | 55 |
| 4% SBSOMMT MB | 1.742 | 0.987 | 0.450 | 66 | 57 | 39 |

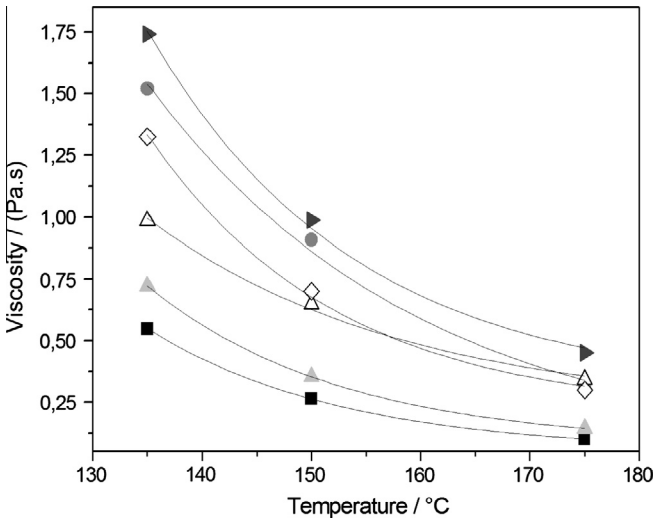


**Fig. 6.** Viscosity as a function of temperature of (■) B, (●) 4%SBS MB, (▲) 4%CLO MB, (△) 4%OMMT MB, (◇) 4%SBSCLO MB, (▶) 4%SBSOMMT MB.

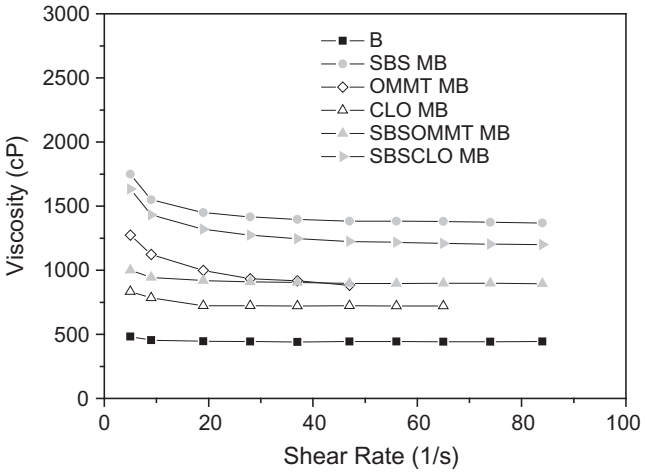


**Fig. 7.** Viscosity as a function of shear rates of (■) B, (●) 4%SBS MB, (▲) 4%SBS OMMT MB, (△) 4% CLO MB, (◇) 4% OMMT MB, (▶) 4% SBSCLO MB.

increase in the viscosity compared to the unmodified bitumen, however less significant. It can be noted that in none of the cases analyzed the viscosity exceeds the Superpave 3 Pa s limit for bitumen measured at 135 °C to guarantee bitumen workability [51]. From the plot of lnη versus (1/t) in Fig. 8, it was obtained the results of flow activation energy, as indicated in the experimental section.

The addition of only SBS or only organoclays resulted in the increase of softening point when compared to the conventional bitumen. However, the nanocomposites SBS/nanoclays showed a decrease in the softening point in relation to the addition of

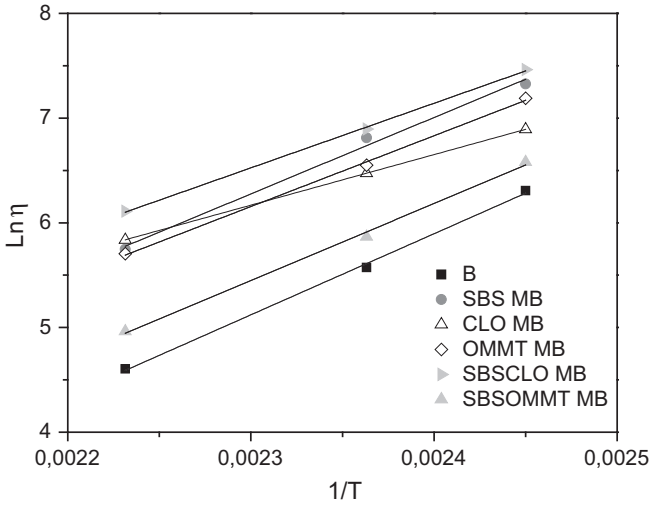


**Fig. 8.** Linear Fit of lnη versus (1/t) of (■) B, (●) 4%SBS MB, (▲) 4%SBS OMMT MB, (△) 4% CLO MB, (◇) 4% OMMT MB, (▶) 4% SBSCLO MB.

individual polymer or organoclays. The softening point changed depending on the type of nanoclay and SBS/nanoclay formed. Probably, it is an indication that the SBS/CLO and SBS/OMMT could be dispersed in a different way in the bitumen. From the results, CLO seemed to present a higher effect than OMMT. This could be due to a better dispersion in the bitumen. In the case of the addition of nanocomposites, it seems that in the blend bitumen/SBS/OMMT, the polymer rich phase is predominantly swelled by the bitumen. The results from bitumen/SBS/CLO suggest that CLO has a better compatibility and the SBS chains were more efficient in intercalating the clay. The discussion presented herein can explain the penetration results in Table 3. The results from SBS/OMMT MB is coherent with the idea that the polymer rich phase is predominantly swelled by the bitumen, and that part of the polymer probably did not interact with the clay.

### 3.4. Rheological properties

#### 3.4.1. Multiple Stress Creep Recovery (MSCR)

Table 4 presents the results for the pure and modified asphalt binders, aged in short term and tested on maximum PG temperature, at 3200 Pa [46].

The sample with 4% OMMT had $J_{nr}$ greater than the maximum values by the classification (4.5 $kPa^{-1}$) [49]. Because of this apparent susceptibility to rutting, this material will not be considered in further discussion. The other samples, except for the one with 4% SBS, have a Standard type traffic classification (S), for which it is specified a number of ESALs (equivalent single axle load of 8.2 tons) below 10 million. The sample with 4% SBS can hold Heavy traffic (classification H), i.e., ESALs above 10 million. Thus the 4% SBS blend presented a lower susceptibility to rutting. It should be pointed out that the bitumens modified by 4% of SBSOMMT and

**Table 4**
Results, PG, MSCR classification (CLA), Recovery (R), Non-recoverable creep compliance ($J_{nr}$) and $J_{nr,diff}$.

| Sample | PG | MSCR (Jnr) | CLA | R, 100 Pa, (%) | R, 3200 Pa, (%) | $J_{nr}$, 100 Pa | $J_{nr}$, 3200 Pa | $J_{nr,diff}$ (%) |
|---|---|---|---|---|---|---|---|---|
| B | 70 | 3.8 | Standard | 3.8 | 0.9 | 3.3 | 3.8 | 13.6 |
| OMMT MB | 70 | 5.9 | – | 3.3 | 0.5 | 5.0 | 5.8 | 17.5 |
| CLO MB | 70 | 3.0 | Standard | 8.1 | 1.0 | 2.4 | 3.0 | 23.2 |
| SBS MB | 76 | 1.5 | Heavy | 13.2 | 12.4 | 1.2 | 1.5 | 24.6 |
| SBSOMMT MB | 82 | 2.7 | Standard | 30.3 | 12.1 | 1.8 | 2.7 | 51.0 |
| SBSCLO MB | 82 | 3.8 | Standard | 40.7 | 4.8 | 1.8 | 3.8 | 109.9 |

by 4% of SBSCLO support a Standard traffic (<10 million ESALs) for a temperature 12 °C above the PG temperature indicated for the conventional bitumen. Table 4 presents the results of the R and the values of $J_{nr}$ for the aged binders in the short term, considering the stress levels of 100 and 3200 Pa [46]. These are also the stress values of the parameter $J_{nr,\ diff}$. This parameter has been incorporated into the Superpave specification (Table 7 of the standard AASHTO M320 [52]) as an indicator of the sensitivity of the material to the increased level of stress. By maintaining the value below a maximum limit (75% in high temperature PG), the asphalt binder will not show high sensitivity to stress and will not be very susceptible to rutting accumulation.

The modifications resulted in higher values of R at 100 Pa and 3200 Pa. Higher recovery percentages is translated into a greater capacity of the asphalt binder to recover the strain after the load application, which in practice translates into lower levels of rutting (plastic strain lowest accumulation). The SBSCLO MB has the highest value of R at 100 Pa. However, under 3200 Pa, SBSCLO MB loses the ability to recover the strain upon the load application, followed by CLO MB. The values range between 4.8 and 40.7% for SBSCLO, reaches 30.3% for SBSOMMT, and does not exceed 14% for other blends. According to Table 4, it is clear that in more severe loading conditions, the formulations suffer significant losses in their ability to recover the total strain during the test, except SBS MB.

Smaller values of $J_{nr}$ are interpreted as smaller susceptibility to the accumulation of plastic strain after the vehicle load and therefore, a lower susceptibility to rutting. The B modified by 4% of SBS has the lowest non-recoverable creep compliance among the materials studied, followed by SBSOMMT MB, CLO MB and SBSCLO MB. Results vary from 1.2 to 1.5 $kPa^{-1}$ for the SBS MB, between 1.8 and 2.7 $kPa^{-1}$ for the SBSOMMT MB, between 2.4 and 3.0 $kPa^{-1}$ for the CLO MB, and between 1.8 and 3.8 $kPa^{-1}$ for the SBSCLO MB.

These results indicate that the asphalt modified binders SBSCLO MB and SBSOMMT MB have susceptibility to rutting similar to conventional bitumen, despite the fact that SBSCLO has two PGs above the conventional bitumen is an indicate on that at 70 °C these materials shall provide superior performance, which enhances the viability of merging these clays to modified binders, while maintaining similar levels of performance.

Table 4 present promising results of SBSOMMT MB, SBSCLO MB and SBS MB, i.e., major elastic recoveries and minor susceptibilities to the accumulation of plastic strain.

In the light of the $J_{nr,diff}$, with the exception of bitumen modified by 4% of SBSCLO, the other bitumen are below the 75% threshold. Thus, these materials are considered suitable for use in paving. The percentage differences present the following sequence: B (13.6), CLO MB (23.2), SBS MB (24.61), SBSOMMT MB (51.0) and SBSCLO MB (109.9).

### 3.4.2. Performance Grade

The DSR protocol was used to determine the PG of the bitumens [43]. The results are shown in Table 4. The SBS nanocomposites modified bitumen presented the best results, which means the binder keeps his properties under a wide range of temperature. The SBS modified binder also presented a higher PG when compared to the unmodified bitumen. CLO MB and OMMT MB did not present any PG improvement.

### 3.4.3 Mixing temperatures by Casola's method

The analyses starts with the master curve (Fig. 9) as indicated in session 3.5. The frequency sweep data was used to construct a master curve (reference temperature of 25 °C) of phase angle versus frequency. The method is based on the observation that the phase angle indicates the elasticity of the bitumen. The frequency that corresponds to the phase angle of 86 °C indicated the transition from the viscous behavior to the viscoelastic one,

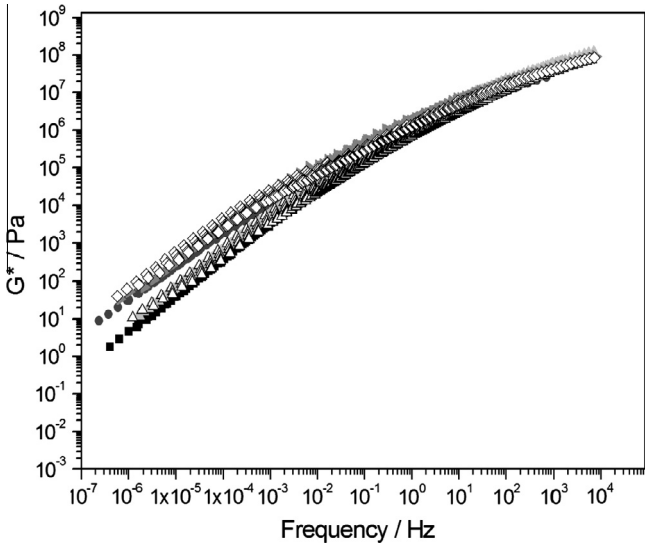


**Fig. 9. Complex modulus** G* as a function of frequency of (■) B, (●) 4%SBS MB, (▲) 4%CLO MB, (△) 4%OMMT MB, (◇) 4%SBSCLO MB, (▶) 4%SBSOMMT MB. Reference temperature of 25 °C.

**Table 5**
Mixing (MT) and compaction temperature (CT).

| Sample | MT (°C) | CT (°C) |
|---|---|---|
| 50/70 B | 152 | 142 |
| 4% SBS MB | 160 | 146 |
| 4% CLO MB | 152 | 142 |
| 4% OMMT MB | 169 | 156 |
| 4% SBSCLO MB | 157 | 147 |
| 4% SBSOMMT MB | 171 | 158 |

and it was correlated to the temperatures at which binders will properly coat the aggregates during mixing (MT) and compaction (CT). These results are indicated at Table 5. As expected, MT and CT of modified bitumens are increased when compared to the unmodified bitumen. The difference between MT and CT was not significant, unless for the case of the OMTT modified bitumens. The results of the flow activation energy (Ef), Table 3, from rotational viscosity of the OMMT modified bitumen were also different from the other modified bitumen, suggesting some different properties, perhaps in compatibility. However, all the values of MT and CT are acceptable to guarantee the workability of the materials.

### 3.5. The effects of nanoclays and SBS/nanoclays modifiers on rheological properties of the bitumen

The frequency dependence of the complex modulus G* for the investigated bitumens is shown in Fig. 9. For all modified bitumens there is an increase in resistance to deformation (G* reflects the total stiffness) when compared to the pure B. This effect is most pronounced at low frequencies (equivalent to high temperatures). SBSOMMT MB, SBSCLO MB, and SBS MB behaved quite similarly, suggesting that the addition of SBS and the combined SBS/nanoclay can result in comparable effects with respect to stiffness, especially at high temperatures where the SBS polymer network is dominant. There is a slight variation when OMMT is added to the bitumen, when compared to the unmodified bitumen.

Fig. 10(a and b) shows rheological parameters G′ and G″ for the studied samples. With respect to the elastic or storage modulus (G′) presented in Fig. 10a, the behavior is slightly different at low frequency (high temperatures) for the SBS modified samples (SBS

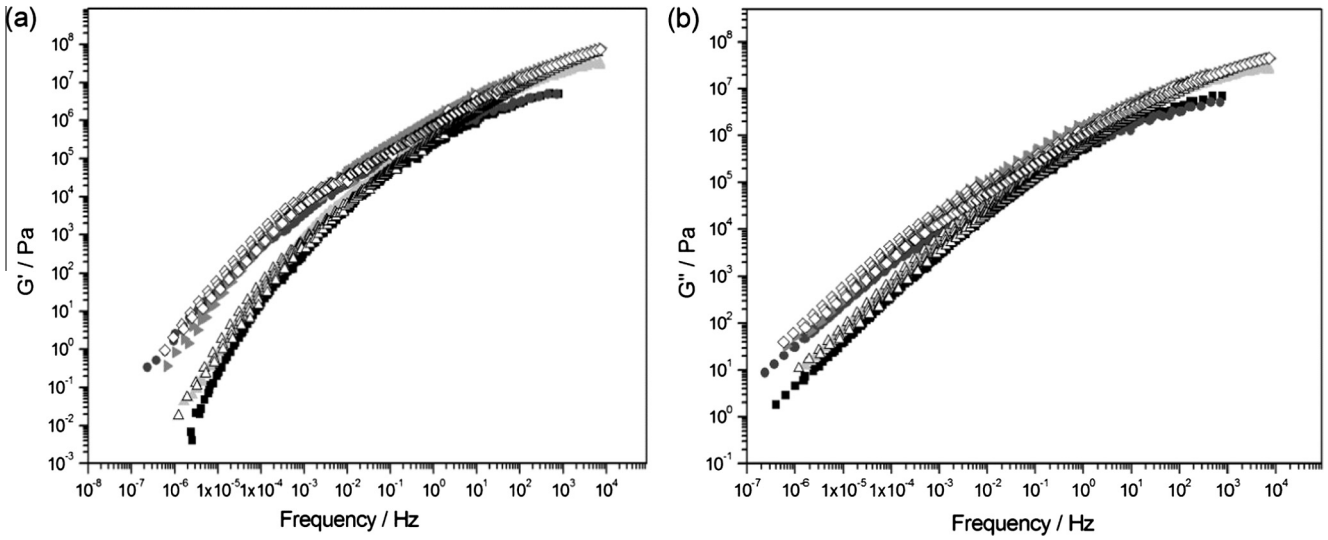


**Fig. 10.** Storage modulus G′ and viscous modulus G″ as a function of frequency of (■) B, (●) 4%SBS MB, (▲) 4%CLO MB, (△) 4%OMMT MB, (◇) 4%SBSCLO MB, (▶) 4%SBSOMMT MB. Reference temperature of 25 °C.

MB, and the nanocomposites SBSCLO MB and SBSOMMT MB) when compared to the other samples. All SBS modified samples showed similar G′ behavior, presenting higher elastic component in relation to the CLO MB and OMMT MB, which present a behavior similar to the unmodified bitumen. The similar rheological behavior observed for the SBS/nanoclay MB and the SBS MB is also an interesting result considering the cost reduction due to the possibility of replacing polymer with clay, without changes in the properties. A rough calculation indicates that the cost reduction would be approximately 36%. According to Sigma-Aldrich Company, the cost of SBS is 280 U$/kg, while the MMT cost is ten times less (2.8 U$/kg).

The loss modulus (G″) of the modified bitumen showed an increase when compared to the G″ of the unmodified bitumen. For all SBS modified samples (Fig. 10b) the viscous component increased in the same order as the complex modulus G* (stiffness) over the entire frequency–temperature domain. The referred samples presented an increase in the loss modulus (stiffness) in relation to the CLO MB and OMMT MB, which remains closer to that of unmodified bitumen. It is also important to consider the possibility of the synergistic effect of the SBS and nanoclays CLO and OMMT. The master curves of G*, G′, G″ indicate that the degree of SBS and SBS/organoclays modification is more pronounced at low frequencies (high temperatures).

The phase angle (δ) as a function of frequency, and the Black diagram for the modified and unmodified bitumens are presented in the δ master curves in Fig. 11(a and b). It is observed that the addition of SBS and the SBS/nanoclays in the bitumen causes a decrease in the phase angle. Such decrease represents an improvement in the elastic response compared to the CLO MB and OMMT MB, and also to the unmodified binder. It can be observed the presence of a δ plateau at intermediate loading frequency-temperature as an indication of a polymer elastic network in the SBS modified samples [10]. The similarity of the plots of δ, as a function of frequency along the entire range for SBS MB and SBS/nanoclays MB, suggests that the effect of these modifiers is quite similar. It is reasonable to conclude that, in terms of rheological parameters, considering the experimental conditions used, all SBS modified samples produce similar effects. It seems that in the case of CLO and OMMT, the nanoclay did not change the elastic response of the SBS modified binder.

The black diagrams were produced because the effects caused by the bitumen modification are highlighted by these diagrams. The behavior of the curves (modified and unmodified bitumens)

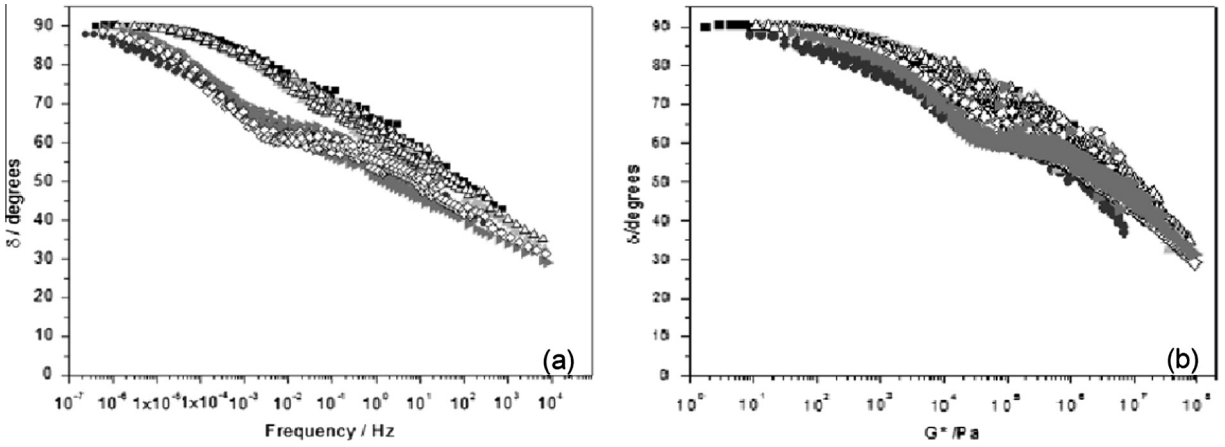


**Fig. 11.** Phase angle δ as a function of frequency and Black diagram of (■) B, (●) 4%SBS MB, (▲) 4%CLO MB, (△) 4%OMMT MB, (◇) 4%SBSCLO MB, (▶) 4%SBSOMMT MB. Reference temperature of 25 °C.

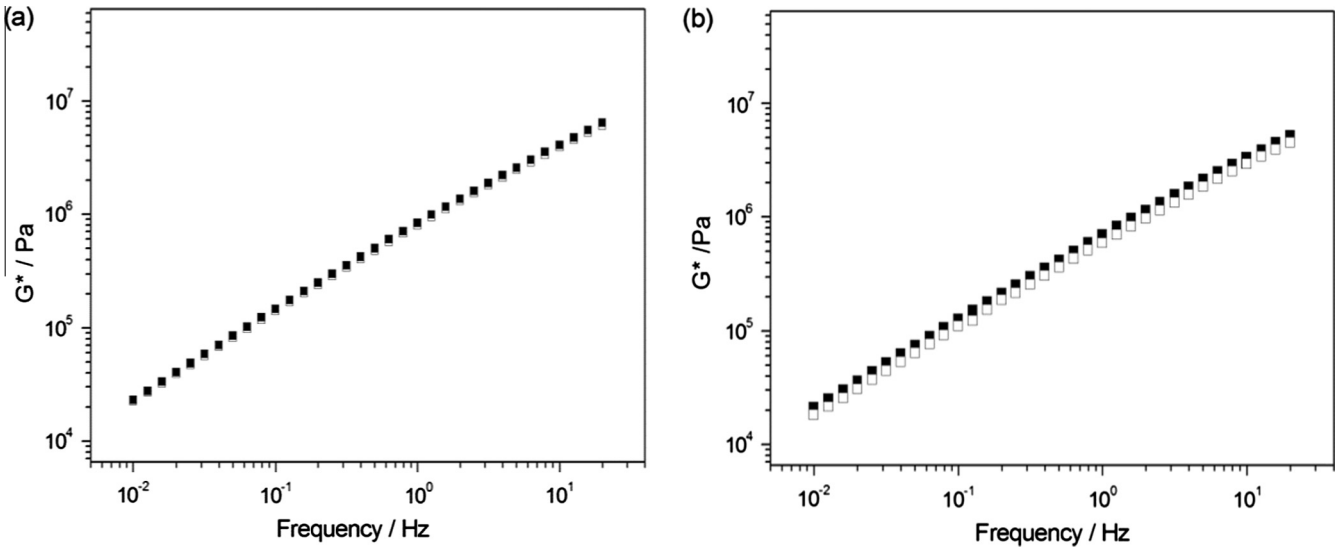


**Fig. 12.** G* as a function of frequency at 25 °C for (■) Top and (□) Bottom MB: (a) 4% CLO MB, (b) 4% OMMT MB.

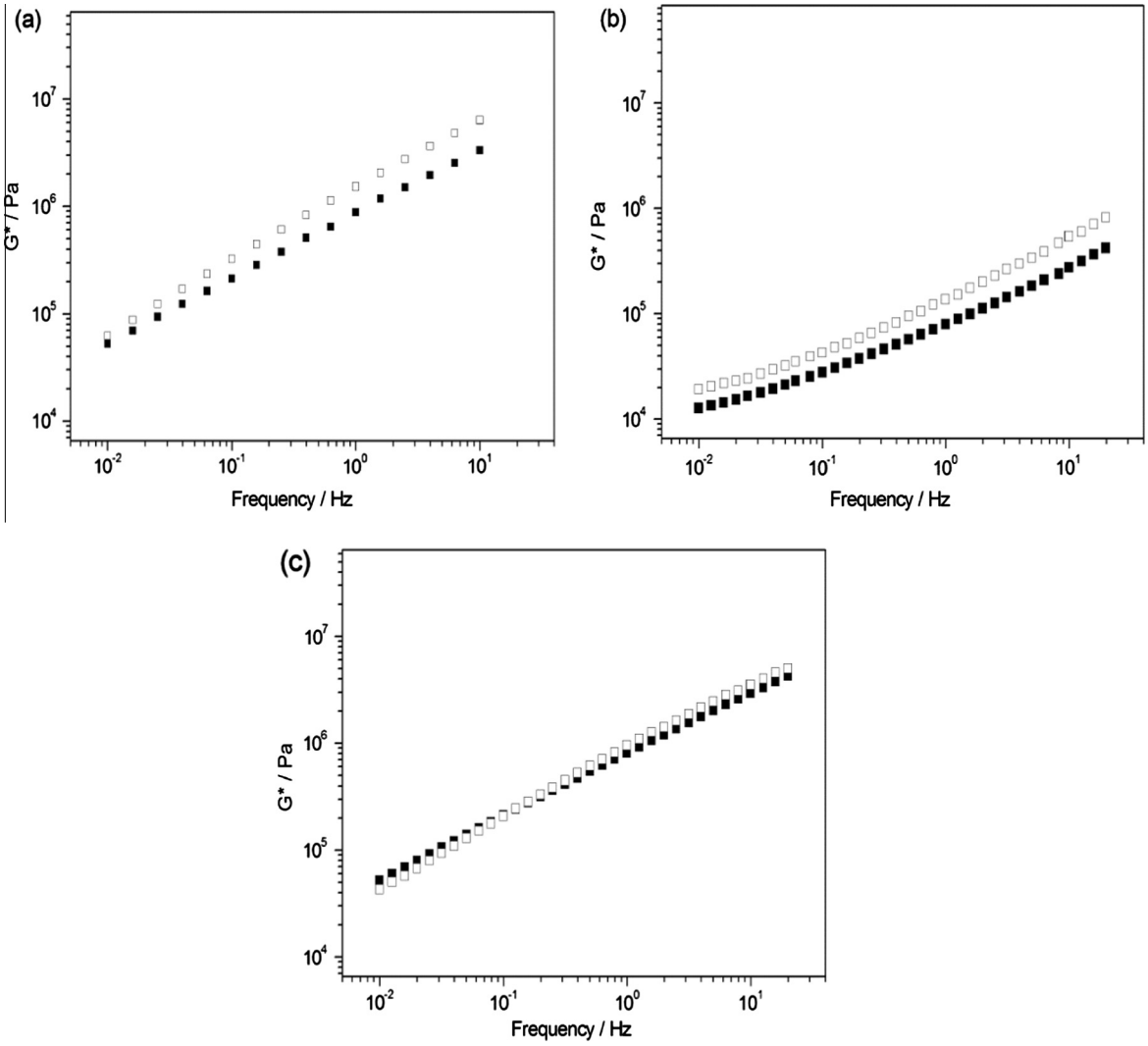


**Fig. 13.** G* as a function of frequency at 25 °C for (■) Top and (□) Bottom MB: (a) 4% SBS MB, (b) 4% SBSOMMT MB, (c) 4% SBSCLO MB.

presented the same pattern – black curves differing only in the magnitude of the parameters. The modification is more significant at intermediate temperatures (equivalent to frequencies from $10^4$ Pa to $10^6$ Pa). At low stiffness values (high temperatures) no significant differences are observed.

### 3.6. Phase separation and storage stability

The phase separation was measured at 60 °C with samples taken from the top and bottom of the test tube. The rheological parameter used was G* obtained from the DSR. Fig. 12(a and b) shows the results of G* as a function of frequency before and after the storage of the samples modified with organoclay.

From the rheological behavior observed in Fig. 12, there is no distinct difference of the G* curves (from the top and the bottom samples) when CLO and OMMT is added, compared to the unmodified bitumen. Fig. 13 presents de results for the samples of top and bottom for the SBS, SBS/OMMT and SBS/CLO nanocomposites.

For the SBS modified bitumen, it was observed the changes in the G* parameter from the top and the bottom samples. G* of the top sample became higher than that of the bottom sample, what indicates a phase separation. There are distinct differences in G* of the two SBS/nanocomposites. It seems that SBS/CLO nanocomposite presents better compatibility with the bitumen when compared to the SBS/OMMT nanocomposite. As shown in the experimental section, in an attempt to improve compatibility, MMT clay was submitted to a surface treatment to produce organophilic clay (OMMT), resulting in an interlayer spacing of 19 Å. Comparing this value with the XRD pattern of CLO (interlayer spacing of 24 Å), it is reasonable to assume that the polymer was more efficiently dispersed in the CLO interlayers than in the OMMT interlayers, leading to a better compatibility and inducing less difference in density relative to the bitumen. Phase separation of SBS/OMMT and the bitumen is probably due to the instability caused by the density difference between them. Taking into account these considerations, it is possible to explain the better performance of SBS/CLO modified bitumen in relation to the storage stability [4].

## 4. Conclusions

The modified bitumens with SBS and SBS/nanoclays exhibited higher complex modulus (G*) and lower phase angle (δ), which implies that these additives improved the resistance to rutting and elasticity of the bitumen. The Performance Grade (PG) of the bitumen modified with SBS/nanoclays composites also presented the best results for preventing major pavement distresses. From the rheological point of view, the OMMT and CLO® modified bitumen showed a similar behavior when compared to the unmodified bitumen. However, the CLO organoclay can improve the high temperature storage stability of the SBS modified bitumen. Comparing 4% of SBS and SBS/nanoclays modification, it seems possible a combination of nanoclay/polymer, leading to savings in the polymer content. There are promising results of SBSOMMT and SBSCLO modified bitumen, presented by the greater elastic recoveries and smaller susceptibilities to the accumulation of plastic deformation. In addition, the bitumen SBSOMMT also presented a resistance to unexpected situations of loading and/or temperature when considering the $J_{nr,diff}$ parameter.

## Acknowledgements

The authors thank Petrobras/Lubnor for the bitumen, and CAPES/Brazil and CNPq/Brazil for their respective supports with scholarships.

## References

[1] M.S. Cortizo, D.O. Larsen, H. Bianchetto, J.L. Alessandrini, Effect of the thermal degradation of SBS copolymers during the ageing of modified asphalts, Polym. Degrad. Stab. 86 (2004) 275–282, http://dx.doi.org/10.1016/j.polymdegradstab.2004.05.006.
[2] Y. Yildirim, Polymer modified asphalt binders, Constr. Build. Mater. 21 (2007) 66–72, http://dx.doi.org/10.1016/j.conbuildmat.2005.07.007.
[3] U. Isacsson, H. Zeng, Low-temperature cracking of polymer-modified asphalt, Mater. Struct. 31 (1998) 58–63, http://dx.doi.org/10.1007/BF02486415.
[4] H. Fu, L. Xie, D. Dou, L. Li, M. Yu, S. Yao, Storage stability and compatibility of asphalt binder modified by SBS graft copolymer, Constr. Build. Mater. 21 (2007) 1528–1533, http://dx.doi.org/10.1016/j.conbuildmat.2006.03.008.
[5] C. Ouyang, S. Wang, Y. Zhang, Y. Zhang, Preparation and properties of styrene-butadiene-styrene copolymer/ kaolinite clay compound and asphalt modified with the compound, Polym. Degrad. Stab. 87 (2005) 309–317, http://dx.doi.org/10.1016/j.polymdegradstab.2004.08.014.
[6] C. Fang, R. Yu, S. Liu, Y. Li, Nanomaterials applied in asphalt modification: a review, J. Mater. Sci. Technol. 29 (2013) 589–594, http://dx.doi.org/10.1016/j.jmst.2013.04.008.
[7] C. Ouyang, S. Wang, Y. Zhang, Y. Zhang, Improving the aging resistance of styrene-butadiene-styrene tri-block copolymer modified asphalt by addition of antioxidants, Polym. Degrad. Stab. 91 (2006) 795–804, http://dx.doi.org/10.1016/j.polymdegradstab.2005.06.009.
[8] H. Yao, Z. You, Nanoclay modified asphalt, in: Innovative Developments of Advanced Multifunctional Nanocomposites in Civil and Structural Engineering, 2016, pp. 183–216.
[9] P.C. Lebaron, Z. Wang, T.J. Pinnavaia, Polymer-layered silicate nanocomposites: an overview, Appl. Clay Sci. 15 (1999) 11–29, http://dx.doi.org/10.1016/S0169-1317(99)00017-4.
[10] M. Biswas, S.S. Ray, Recent progress in synthesis and evaluation of polymer-montmorillonite nanocomposites, Adv. Polym. Sci. 155 (2001) 167–221, http://dx.doi.org/10.1007/3-540-44473-4_3.
[11] A. Usuki, Y. Kojima, M. Kawasumi, A. Okada, Y. Fukushima, Synthesis of nylon 6-clay hybrid, J. Mater. Res. 1993 (1993) 1179–1185, http://dx.doi.org/10.1557/JMR.1993.1179.
[12] R.A. Vaia, G. Price, P.N. Ruth, H.T. Nguyen, J. Lichtenhan, Polymer/layered silicate nanocomposites as high performance ablative materials, Appl. Clay Sci. 15 (1999) 67–92, http://dx.doi.org/10.1016/S0169-1317(99)00013-7.
[13] E.P. Giannelis, Polymer layered silicate nanocomposites, Adv. Mater. 8 (1996) 29–35, http://dx.doi.org/10.1002/adma.19960080104.
[14] E.P. Giannelis, Polymer-layered silicate nanocomposites: synthesis, properties and applications, Appl. Organomet. Chem. 12 (1998) 675–680. doi:10.1002/(SICI)1099-0739(199810/11)12:10/11<675::AID-AOC779>3.0.CO;2-V..
[15] R.K. Bharadwaj, Modeling the barrier properties of polymer-layered silicate nanocomposites, Macromolecules 34 (2001) 9189–9192, http://dx.doi.org/10.1021/ma010780b.
[16] K. Yano, A. Usuki, A. Okada, T. Kurauchi, O. Kamigaito, Synthesis and properties of polyimide-clay hybrid, J. Polym. Sci., Part A: Polym. Chem. 31 (1993) 2493–2498, http://dx.doi.org/10.1002/pola.1993.080311009.
[17] P.B. Messersmith, E.P. Giannelis, Synthesis and barrier properties of poly(ε-caprolactone)-layered silicate nanocomposites, J. Polym. Sci., Part A: Polym. Chem. 33 (1995) 1047–1057, http://dx.doi.org/10.1002/pola.1995.080330707.
[18] Y. Kojima, A. Usuki, M. Kawasumi, A. Okada, Y. Fukushima, T. Kurauchi, O. Kamigaito, Mechanical properties of nylon 6-clay hybrid, J. Mater. Res. 8 (2011) 1185–1189, http://dx.doi.org/10.1557/JMR.1993.1185.
[19] N. Biomedical, R. Xu, E. Manias, New biomedical poly(urethane urea)-layered silicate nanocomposites, Notes (2001) 337–339, http://dx.doi.org/10.1021/ma0013657.
[20] J. Gilman, Flammability and thermal stability studies of polymer layered-silicate (clay) nanocomposites, Appl. Clay Sci. 15 (1999) 31–49, http://dx.doi.org/10.1016/S0169-1317(99)00019-8.
[21] J.W. Gilman, T. Kashiwagi, J.D. Lichtenhan, Nanocomposites: a revolutionary new flame retardant approach, SAMPE J. 33 (1997) 40–46. <Go to ISI>://WOS:A1997XK81000007.
[22] J.W. Gilman, C.L. Jackson, A.B. Morgan, R. Harris, E. Manias, E.P. Giannelis, M. Wuthenow, D. Hilton, S.H. Phillips, Flammability properties of polymer – Layered-silicate nanocomposites. Polypropylene and polystyrene nanocomposites, Chem. Mater. 12 (2000) 1866–1873, http://dx.doi.org/10.1021/cm0001760.
[23] S. Bourbigot, M. Le Bras, F. Dabrowski, J.W. Gilman, T. Kashiwagi, PA-6 clay nanocomposite hybrid as char forming agent in intumescent formulations, Fire Mater. 24 (2000) 201–208. doi:10.1002/1099-1018(200007/08)24:4<201::AID-FAM739>3.0.CO;2-D..
[24] F. Dabrowski, L. Bras, S. Bourbigot, J.W. Gilman, T. Kashiwagi, in: Proceedings of the Eurofillers '99, Lyon-Villeurbanne, France, 1999, pp. 6–9 (n.d.).
[25] J.C. Miranda-Trevino, C.A. Coles, Kaolinite properties, structure and influence of metal retention on pH, Appl. Clay Sci. 23 (2003) 133–139, http://dx.doi.org/10.1016/S0169-1317(03)00095-4.
[26] T.F. Pamplona, B. De, A.E.V. De Alencar, A.P.D. Lima, N.M.P.S. Ricardo, J.B. Soares, S. De, Asphalt binders modified by SBS and SBS/nanoclays: effect on rheological properties, J. Braz. Chem. Soc. 23 (2012) 639–647.
[27] P. Henrique, C. Camargo, K.G. Satyanarayana, F. Wypych, Nanocomposites: synthesis, structure, properties and new application opportunities, Mater. Res. 12 (2009) 1–39, http://dx.doi.org/10.1590/S1516-14392009000100002.

[28] M.S. Lakshmi, M. Sriranjani, H.B. Bakrudeen, A.S. Kannan, A.B. Mandal, B.S.R. Reddy, Carvedilol/montmorillonite: processing, characterization and release studies, Appl. Clay Sci. 48 (2010) 589–593, http://dx.doi.org/10.1016/j.clay.2010.03.008.
[29] M. Alexandre, P. Dubois, Polymer-layered silicate nanocomposites: preparation, properties and uses of a new class of materials, Mater. Sci. Eng. R Rep. 28 (2000) 1–63, http://dx.doi.org/10.1016/S0927-796X(00)00012-7.
[30] G.I. Nakas, C. Kaynak, Use of different alkylammonium salts in clay surface modification for epoxy-based nanocomposites, Polym. Compos. 30 (2009) 357–363, http://dx.doi.org/10.1002/pc.20667.
[31] A. Rehab, N. Salahuddin, Nanocomposite materials based on polyurethane intercalated into montmorillonite clay, Mater. Sci. Eng., A 399 (2005) 368–376, http://dx.doi.org/10.1016/j.msea.2005.04.019.
[32] J. Yu, X. Wang, D. Kuang, H. Zhang, Effect of organophilic montmorillonite on thermal-oxidative aging behavior of SBS modified bitumen crack filling material, J. Wuhan Univ. Technol. Mater. Sci. Ed. 24 (2009) 673–676, http://dx.doi.org/10.1007/s11595-009-4673-9.
[33] Y.-P. Huang, T.-Y. Tsai, W. Lee, W.-K. Chin, Y.-M. Chang, H.-Y. Chen, Photorefractive effect in nematic-clay nanocomposites, Opt. Express 13 (2005) 2058–2063, http://dx.doi.org/10.1364/OPEX.13.002058.
[34] S. Lee, Microstructure, tensile properties, and biodegradability of aliphatic polyester/clay nanocomposites, Polymer (Guildf) 43 (2002) 2495–2500, http://dx.doi.org/10.1016/S0032-3861(02)00012-5.
[35] M. Önal, Y. Sarikaya, Some physicochemical properties of methylammonium and ethylenediammonium smectites, Colloids Surf., A (2008), http://dx.doi.org/10.1016/j.colsurfa.2007.06.023.
[36] K.P. Kitsopoulos, Cation-exchange capacity (CEC) of zeolitic volcaniclastic materials: applicability of the ammonium acetate saturation (AMAS) method, Clays Clay Miner. (1999), http://dx.doi.org/10.1346/CCMN.1999.0470602.
[37] ASTM D4402, Standard Test Method for Viscosity Determinations of Unfilled Asphalts using Brookfield Thermosel Apparatus, Philadelphia, 2002, (n.d.).
[38] ASTM D5, Standard Test Method for Penetration of Bituminous Materials, Philadelphia, 2005.pdf, (n.d.).
[39] ASTM D36, Standarad test method for Softening point of Bitumen (Ring and Ball Apparatus), West Conshohocken, 2009, (n.d.).
[40] ASTM D7175, Standard Test Method for Determining the Rheological Properties of Asphalt Binder using a Dynamic Shear Rheometer, Philadelphia, 2005 ASTM D6373; Standard Specification for Performance Graded Asphalt Binder, West Conshohocken, 2007, (n.d.).
[41] J.P. Pfeiffer, P.M. Van Doormal, J. Inst. Pet. 22 (1936). 414.pdf, (n.d.)..
[42] ASTM D6373, Standard Specification for Performance Graded Asphalt Binder, West Conshohocken, 2007, (2007) p. 6373.
[43] R. West, D. Watson, P. Turner, J. Casola, Mixing and compaction temperatures of apshalt binders in hot-mix, Asphalt (2010).
[44] ASTM D7405, Standard Test Method for Multiple Stress Creep and Recovery (MSCR) of Asphalt Binder Using a Dynamic Shear Rheometer, West Conshohocken, 2010, (n.d.).
[45] M. Anderson, 54th Annual Idaho Asphalt Conference, 2014.
[46] G.A. Harder, 54th Annual Pennsylvania Asphalt Conference, 2014.
[47] K. Adorjányi, P. Füleki, Correlation between permanent deformation-related performance parameters of asphalt concrete mixes and binders, Open Eng. 3 (2013), http://dx.doi.org/10.2478/s13531-012-0073-6.
[48] J.A. D'Angelo, The Relationship of the MSCR Test to Rutting, Road Mater. (1999) 31–49, http://dx.doi.org/10.1016/S0169-1317(99)00019-8.
[49] J.A. D'Angelo, The relationship of the MSCR test to rutting, Road Mater. Pavement Des. 10 (2009) 61–80, http://dx.doi.org/10.1080/14680629.2009.9690236.
[50] ABNT NBR 15166, Asfalto Modificado; Ensaio de Separação de Fase, Rio de Janeiro, Brasil, 2004.
[51] Y. Richard Kim, Modeling of Asphalt Concrete, Complex Modulus from the Indirect Tension Test, Chapter (McGraw-Hill Professional, 2009), Access Engineering.
[52] AASHTO M320, Standard Specification for Performance Graded Asphalt Binder, Washington, 2009, (n.d.).